

Atomistic-Scale Simulations of the Initial Chemical Events in the Thermal Initiation of Triacetoneperoxide

Adri C. T. van Duin,^{*,†} Yehuda Zeiri,^{‡,§} Faina Dubnikova,[‡] Ronnie Kosloff,[‡] and William A. Goddard, III[†]

Contribution from the Materials and Process Simulation Center, California Institute of Technology, Pasadena, California 91125, Fritz Haber Center for Molecular Dynamics, Hebrew University, Jerusalem 91904, Israel, and Chemistry Department, NRCN, P.O. Box 9001, Beer-Sheva 84190, Israel

Received March 31, 2005; E-mail: duin@wag.caltech.edu

Abstract: To study the initial chemical events related to the detonation of triacetoneperoxide (TATP), we have performed a series of molecular dynamics (MD) simulations. In these simulations we used the ReaxFF reactive force field, which we have extended to reproduce the quantum mechanics (QM)-derived relative energies of the reactants, products, intermediates, and transition states related to the TATP unimolecular decomposition. We find excellent agreement between the QM-predicted reaction products and those observed from 100 independent ReaxFF unimolecular MD cookoff simulations. Furthermore, the primary reaction products and average initiation temperature observed in these 100 independent unimolecular cookoff simulations match closely with those observed from a TATP condensed-phase cookoff simulation, indicating that unimolecular decomposition dominates the thermal initiation of the TATP condensed phase. Our simulations demonstrate that thermal initiation of condensed-phase TATP is entropy-driven (rather than enthalpy-driven), since the initial reaction (which mainly leads to the formation of acetone, O₂, and several unstable C₃H₆O₂ isomers) is almost energy-neutral. The O₂ generated in the initiation steps is subsequently utilized in exothermic secondary reactions, leading finally to formation of water and a wide range of small hydrocarbons, acids, aldehydes, ketones, ethers, and alcohols.

1. Introduction

The peroxide-based explosives, including triacetoneperoxide (TATP, Figure 1) and diacetonediperoxide (DADP), have found few civilian or military applications^{1,2} due to their low chemical stability, sensitivity to mechanical stress, and high volatility. Unfortunately, the straightforward synthesis of these explosives from readily available materials has made them popular components of explosive devices improvised by terrorists worldwide. As such, there is a great demand for analytical methodology capable of detecting these materials³ and for designing additives that could improve their detection possibilities. To develop such methodology, an understanding of the initial chemical events leading to the detonation is critical. The explosive nature of these peroxides hampers a detailed experimental study of these initiation steps, and as such experimental observations on peroxide-based materials are limited to analysis of post-blast residues or thermal decomposition studies.^{4–6} An alternative to such experimental studies is atomistic-scale

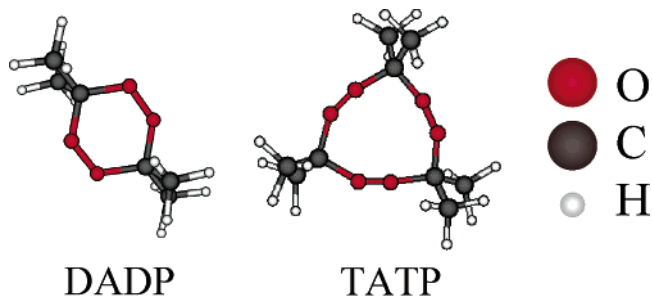


Figure 1. DADP and TATP structures with definition of the atom color conventions.

computational simulation methods that do, in principle, allow us to obtain the femtosecond-scale resolution required to study these initiation events. Indeed, quantum mechanics (QM) methods have been successfully employed to study several possible unimolecular TATP-decomposition pathways⁷ and, as such, have provided valuable insights into the chemistry of these materials. Unfortunately, the computational expense of these QM methods makes them less practical for studying the high-temperature initiation events in condensed-phase materials. Empirical force field (FF) methods are many orders of magnitude faster than QM methods and as such can be applied to

[†] California Institute of Technology.

[‡] Hebrew University.

[§] NRCN.

- (1) Milas, N. A.; Golubovic, N. *J. Am. Chem. Soc.* **1959**, *91*, 6459.
- (2) Evans, H. E.; Tulleners, F. A. J.; Sanchez, B. L.; Rasmussen, C. A. *J. Forensic Sci.* **1986**, *31*, 1119.
- (3) Dubnikova, F.; Kosloff, R.; Zeiri, Y.; Karpas, Z. *J. Phys. Chem. A* **2002**, *106*, 4951.
- (4) Sanderson, J. R.; Story, P. R. *J. Org. Chem.* **1974**, *39*, 3463.
- (5) Eyler, G. N.; Canizo, A. I.; Alvarez, E. E.; Cafferata, L. F. *R. An. Asoc. Quim. Argent.* **1994**, *82*, 175.

(6) Oxley, J. C.; Smith, J. L.; Chen, H. *Propellants, Explos., Pyrotech.* **2002**, *27*, 209.

(7) Dubnikova, F.; Kosloff, R.; Almog, J.; Zeiri, Y.; Boese, R.; Itzhaky, H.; Alf, A.; Keinan, E. *J. Am. Chem. Soc.* **2005**, *127*, 1146.

molecular dynamics (MD) studies on relatively large ($\gg 1000$ atoms) systems, but most FF methods are applicable only to systems close to their equilibrium geometry and do not properly describe the energetics related to the dissociation and formation of chemical bonds.

Recently, we developed ReaxFF, an FF method capable of describing reactions. ReaxFF is based on the bond order/bond distance concept introduced in force field methods by Tersoff⁸ and initially applied to hydrocarbons by Brenner.⁹ We found that ReaxFF can reproduce QM energies for reactive systems, including reactants, transition states, and products, for a wide range of materials, including hydrocarbons,¹⁰ nitramines,^{11,12} silicon/silicon oxides,^{13,14} aluminum/aluminum oxides,¹⁵ transition metal interactions with first-row elements,¹⁶ and magnesium/magnesium hydrides.¹⁷

To enable a high-temperature reactive dynamical study of condensed-phase TATP, we added the QM data reported earlier for the TATP unimolecular pathways⁷ to the ReaxFF nitramines training set and reoptimized the ReaxFF parameters to obtain a force field that describes both nitramines and alkyl cyclic peroxides. We subsequently applied this ReaxFF to study the differences between unimolecular and condensed-phase TATP thermal initiation and to analyze the nature and energetics of the related primary and secondary products.

2. Methods

2.1. ReaxFF. ReaxFF employs instantaneous bond orders (BO'_{ij}), including contributions from σ , π , and double- π bonds, which are calculated from the interatomic distances (r_{ij}) using eq 1; these instantaneous bond orders are subsequently corrected with overcoordination and undercoordination terms to force systems toward the proper valency. These bond orders are updated every MD iteration, thus allowing ReaxFF to recognize new bonds and to break existing bonds.

$$BO'_{ij} = BO_{ij}^{\sigma} + BO_{ij}^{\pi} + BO_{ij}^{\pi\pi} = \exp\left[p_{bo1} \cdot \left(\frac{r_{ij}}{r_o^{\sigma}}\right)^{p_{bo2}}\right] + \exp\left[p_{bo3} \cdot \left(\frac{r_{ij}}{r_o^{\pi}}\right)^{p_{bo4}}\right] + \exp\left[p_{bo5} \cdot \left(\frac{r_{ij}}{r_o^{\pi\pi}}\right)^{p_{bo6}}\right] \quad (1)$$

ReaxFF partitions the overall system energy into contributions from various partial energy terms (eq 2). These partial energies include bond order-dependent terms such as bond energies, valence angle, lone pair, conjugation, and torsion angle terms to properly handle the nature of preferred configurations of atomic and resulting molecular orbitals, and bond order-independent terms that handle nonbonded van der Waals and Coulombic interactions. These nonbonded interactions are calculated between every atom pair, irrespective of connectivity, and are shielded to avoid excessive repulsion at short distances. In addition, the charges of the atoms depend continuously on the geometry using general expressions based on atom electronegativity and hardness,

- (8) Tersoff, J. *Phys. Rev. B* **1988**, *38*, 9902.
 (9) Brenner, D. W. *Phys. Rev. B* **1990**, *42*, 9458.
 (10) van Duin, A. C. T.; Dasgupta, S.; Lorant, F.; Goddard, W. A., III. *J. Phys. Chem. A* **2001**, *105*, 9396.
 (11) Strachan, A.; van Duin, A. C. T.; Chakraborty, D.; Dasgupta, S.; Goddard, W. A., III. *Phys. Rev. Lett.* **2003**, *91*, 098301.
 (12) Strachan, A.; Kober, E.; van Duin, A. C. T.; Oxgaard, J.; Goddard, W. A., III. *J. Chem. Phys.* **2005**, *122*, 054502.
 (13) van Duin, A. C. T.; Strachan, A.; Stewman, S.; Zhang, Q.; Xu, X.; Goddard, W. A., III. *J. Phys. Chem. A* **2003**, *107*, 3803.
 (14) Chenoweth, K.; Cheung, S.; van Duin, A. C. T.; Goddard, W. A., III; Kober, E. M. *J. Am. Chem. Soc.* **2005**, *127*, 7192.
 (15) Zhang, Q.; Cagin, T.; van Duin, A. C. T.; Goddard, W. A., III; Qi, Y.; Hector, L. *Phys. Rev. B* **2004**, *69*, 045423.
 (16) Nielson, K.; van Duin, A. C. T.; Oxgaard, J.; Deng, W.; Goddard, W. A., III. *J. Phys. Chem. A* **2005**, *109*, 493.
 (17) Cheung, S.; Deng, W.; van Duin, A. C. T.; Goddard, W. A., III. *J. Phys. Chem. A* **2005**, *109*, 851.

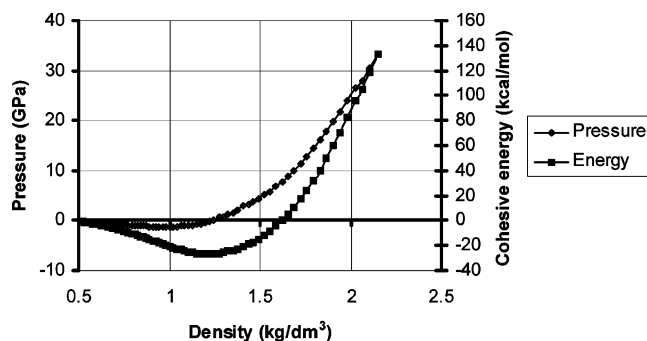


Figure 2. ReaxFF energy/volume and pressure/volume relation for the TATP crystal.

whose parameters are also derived from QM. This treatment of nonbonded interactions allows ReaxFF to describe covalent, ionic, and intermediate materials with the same parameters, thus greatly enhancing its transferability.

$$E_{\text{system}} = E_{\text{bond}} + E_{\text{lp}} + E_{\text{over}} + E_{\text{under}} + E_{\text{val}} + E_{\text{pen}} + E_{\text{coa}} + E_{\text{C2}} + E_{\text{tors}} + E_{\text{conj}} + E_{\text{H-bond}} + E_{\text{vdWaaals}} + E_{\text{Coulombic}} \quad (2)$$

For a more detailed description of these partial energy terms, see refs 10 and 16.

2.2. Molecular Dynamics Simulations. All simulations and force field optimizations were performed using the ReaxFF program,¹⁸ which carries out both MD simulations and force field optimization using the ReaxFF system energy description. A Berendsen thermostat and barostat¹⁹ were used to control the temperature and pressure in the NVT and NPT simulations.

Single-Molecule Cookoff Simulations. To simulate the temperature-induced dissociation of the single TATP molecule, we put 1 TATP molecule in a $15 \times 15 \times 15 \text{ \AA}^3$ periodic box (density 0.109 kg/dm^3). This system was energy-minimized and subsequently equilibrated at $T = 300 \text{ K}$ in a 25-ps NVT/MD simulation with a time step of 0.25 fs and a temperature damping constant of 500 fs. After this equilibration was run, 100 decoupled configurations were generated for this system by performing 125-ps NVT/MD simulations under equilibrium conditions and saving atom positions and velocity distributions every 1.25 ps. For each of these 100 configurations, a cookoff simulation was performed. In these cookoff simulations a time step of 0.25 fs was used with a temperature damping constant of 500 fs. The target system temperature was raised continuously by 0.05 K/MD iteration (equivalent to a heating rate of 200 K/ps) during a 12.5-ps simulation, resulting in a final target temperature of 2800 K. This heating period is comparable with the time a shock wave passes a distance of a few unit cells in the crystal during detonation, assuming a shock wave velocity of about 2000–5000 m/s ($=20\text{--}50 \text{ A/ps}$). As a result of the rapid heating and the fairly high temperature damping constant the system temperature is always lagging behind the target temperature by an average of 180 K (see Figures 4 and 5). System configurations were saved every 0.125 ps and were analyzed for molecular composition, using the ReaxFF-derived bond orders to identify molecular fragments; any fragments that were not connected by a bond with a ReaxFF bond order larger than 0.3 were considered separate molecules. Note that the ReaxFF methodology does not use this molecular information in any way in the system energy evaluation; we only use the ReaxFF bond orders as a convenient tool to perform the fragment analysis.

Condensed-Phase Cookoff Simulations. To simulate the temperature-induced initiation of a TATP condensed phase, we performed simulations on a 32-molecule TATP crystal supercell (cell parameters

- (18) The ReaxFF program is available for distribution to academic users. Please contact A.C.T.v.D. (duin@wag.caltech.edu) or W.A.G. (wag@wag.caltech.edu).
 (19) Berendsen, H. J. C.; Postma, J. P. M.; van Gunsteren, W. F.; DiNola, A.; Haak, J. R. *J. Chem. Phys.* **1984**, *81*, 3684.

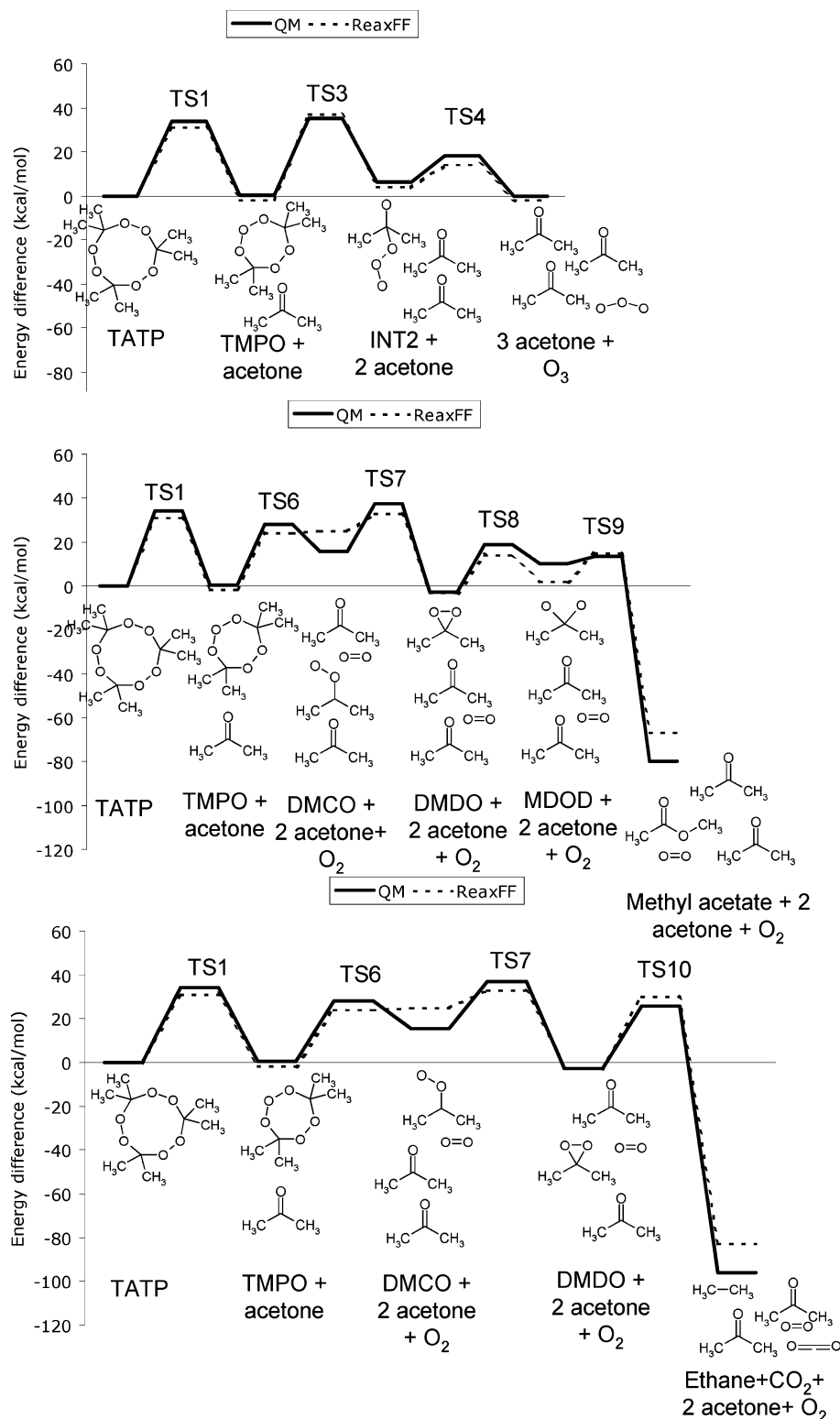


Figure 3. QM and ReaxFF energies for three TATP unimolecular dissociation pathways. For a description of the transition state geometries (TS1 through TS10), see Dubnikova et al.⁷ The following shorthand notations were used above: 4,4,7,7-tetramethyl-1,2,3,5,6-pentoxepane is noted as TMPO, dimethyldioxacyclopropane is noted as DMDO, and dimethylcarbonyl oxide is noted as DMCO.

$a = 27.576 \text{ \AA}$, $b = 21.328 \text{ \AA}$, $c = 15.788 \text{ \AA}$, $\alpha = 90^\circ$, $\beta = 91.775^\circ$, $\gamma = 90^\circ$, density = 1.272 kg/dm^3 , calculated cohesive energy⁷ (Dreiding FF) -21.61 kcal/mol , $T = 180 \text{ K}$. This supercell was constructed from the X-ray structure obtained by Dubnikova et al.⁷ To test the ReaxFF description of the TATP condensed phase, we determined the ReaxFF energy/volume and pressure/volume relation for this TATP supercell (Figure 2); we found that ReaxFF obtains an equilibrium density of

1.222 kg/dm^3 and a cohesive energy of -26.7 kcal/mol . We also performed an NPT simulation at $P = 1 \text{ bar}$ and $T = 180 \text{ K}$ and found that the ReaxFF crystal volume, symmetry, and cell parameters are in good agreement with experiment. The 32-molecule supercell was equilibrated at 300 K during a 25-ps MD/NVT simulation (time step 0.25 fs , temperature damping constant 500 fs) and was subsequently subjected to the same temperature program as that employed in the

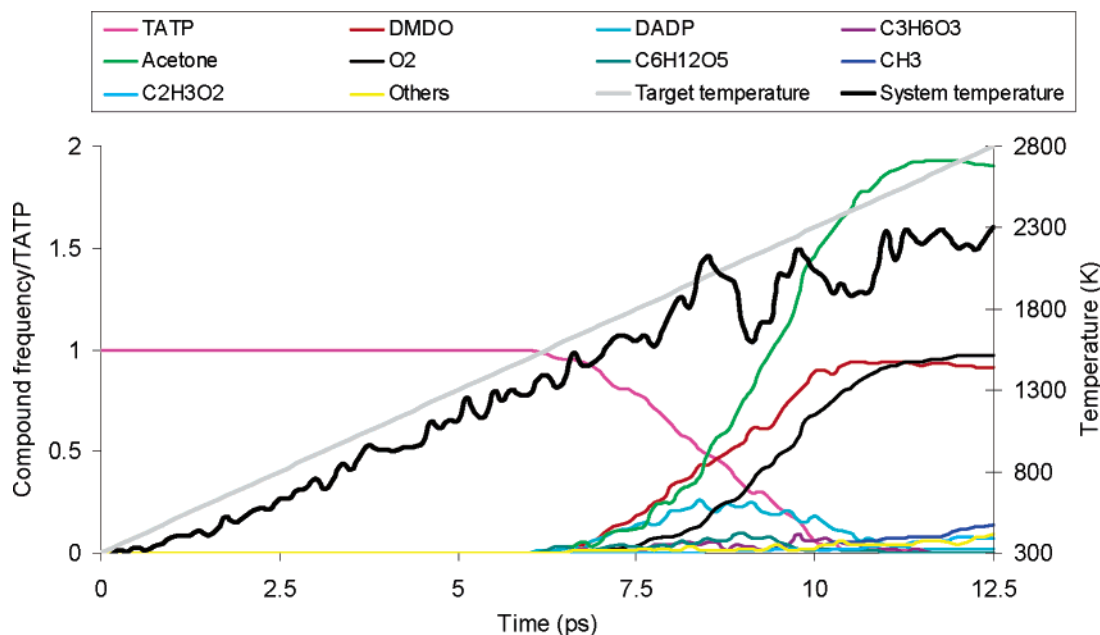


Figure 4. Average product distribution obtained from 100 independent cookoff simulations on isolated TATP molecules. Only major products are shown explicitly; all minor products are summed in “Others”.

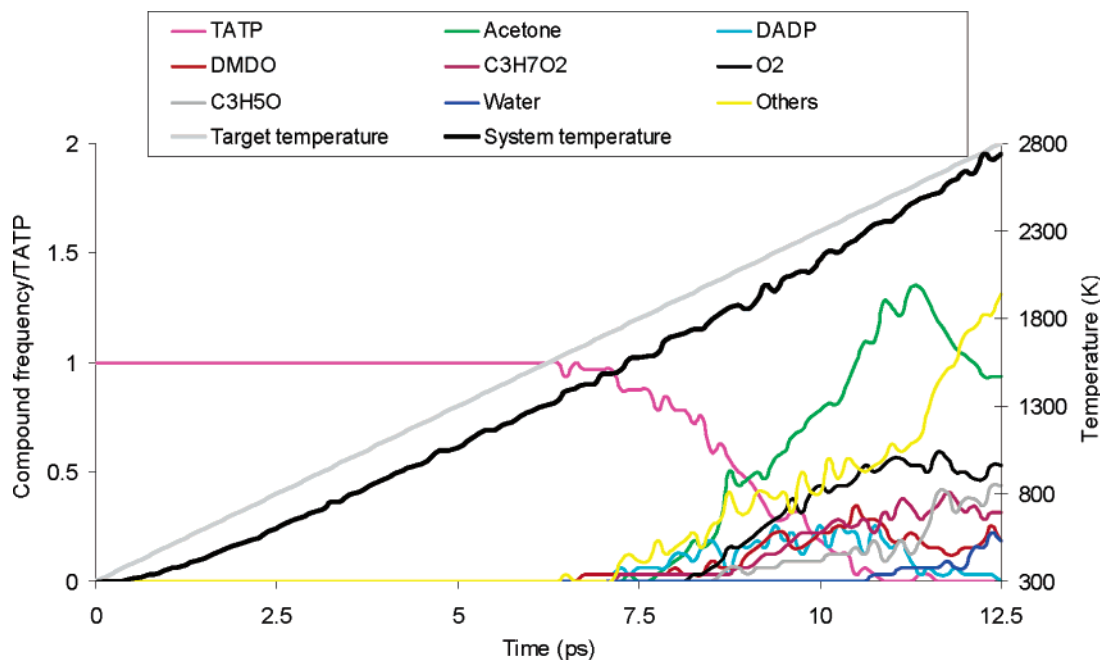


Figure 5. Products observed in the cookoff simulation of condensed-phase TATP (32 monomers; density = 1.272 kg/dm³). Only major products are shown explicitly; all minor products are summed in “Others”.

single-molecule cookoff (continuous temperature increase by 200 K/ps during a 12.5-ps simulation, taking the target temperature from 300 to 2800 K). To test the effects of heating rate on the observed initiation temperature we also performed a 62.5-ps simulation with a heating rate of 40 K/ps. The extended cookoff simulations were started from the same 300 K equilibrated configuration, which was heated to $T = 1800$ K during the first 7.5 ps and was subsequently kept at $T = 1800$ K for the rest of the simulation (another 142.5 ps). The NVE simulation was initiated from a configuration obtained from the NVT cookoff simulations in which the system temperature had reached $T = 1250$ K. To ensure good energy conservation during the NVE simulations, we used a time step of 0.05 fs. The NVE simulation was performed for 176.5 ps, at which stage the energy-releasing TATP secondary reactions were finished.

3. Results and Discussion

3.1. Force Field Development. To develop a ReaxFF description of TATP chemistry, we added QM data for TATP unimolecular decomposition, obtained by Dubnikova et al.⁷ at the DFT:B3LYP/cc-pVDZ level of theory, to the nitramines training set that was used to derive the force field employed to simulate shock decomposition of RDX.¹¹ In addition to the TATP and RDX-specific data, this training set contains a wide range of general data, including all hydrocarbon data from ref 10, charge distributions, bond dissociation energies for all single, double, and triple H–H, C–H, C–C, C–N, N–H, N–N, N–O,

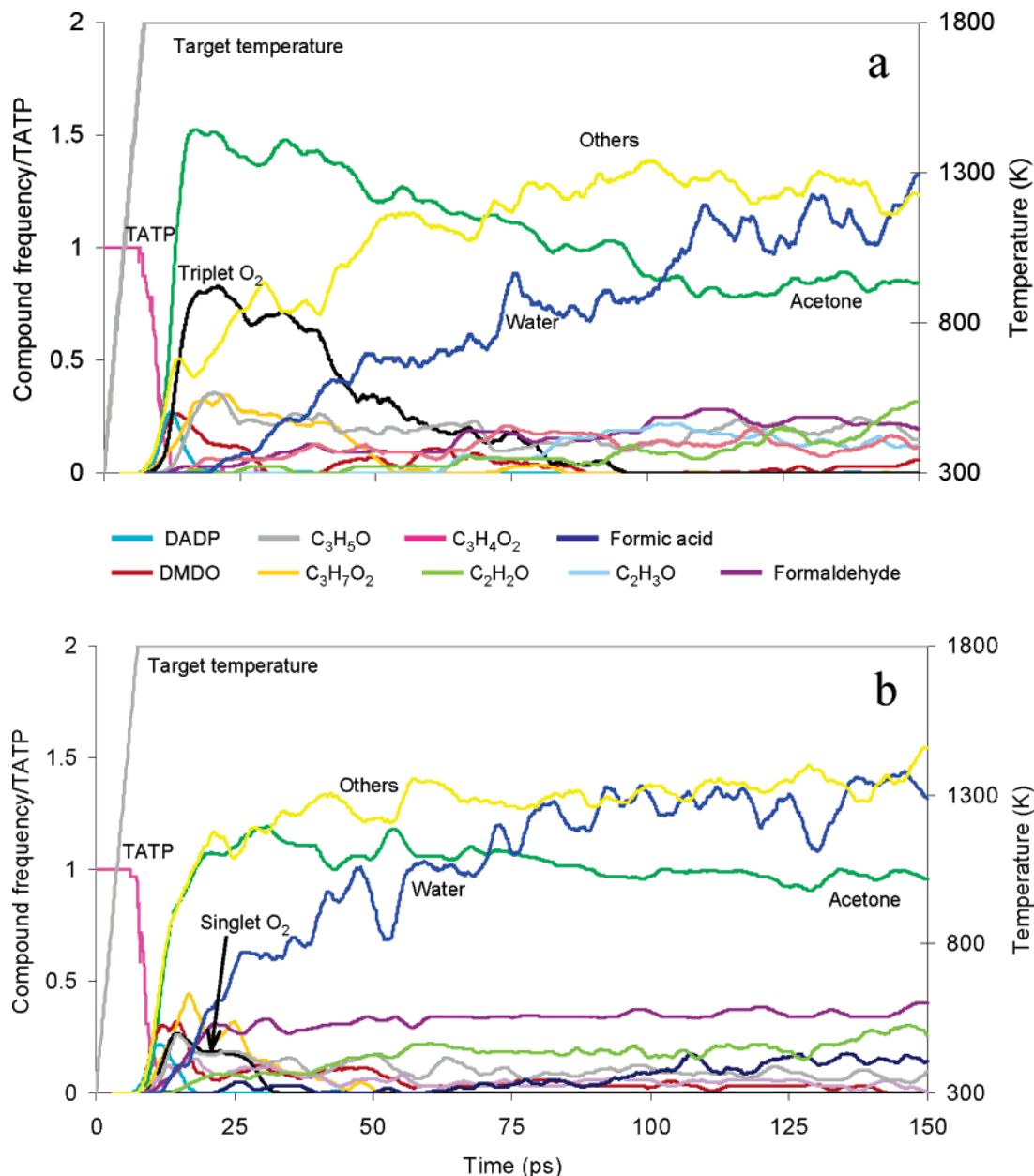


Figure 6. Products observed in solid TATP cookoff using force fields based on O_2 triplet (a) and O_2 singlet (b) O–O dissociation energies. Only major products are shown explicitly; all minor products are summed in “Others”.

and O–O bonds, relative stabilities of a wide range of small molecules (including species relevant to TATP secondary chemistry such as H_2O , H_2O_2 , CO_2 , CO , O_2 , O_3 , methanol, and formic acid), angle distortion energies for all H-, C-, N-, and O-containing valence angles, rotational barriers around every relevant single and double bond, vibrational frequencies for a range of small molecules and densities, equations of state, and cohesive energies for various molecular crystals. Furthermore, the training set contains reaction barriers for hydrogen transfers and radical rearrangements that might play a part in the TATP secondary reactions. To ensure a reliable description of the attractive nonbonded interactions, we fitted the ReaxFF cohesive energies of the molecular crystals to experimental rather than to QM data

Due to the size and the chemical diversity of the training set, we believe that the force field resulting from the parameter

optimization against these data should be applicable beyond the scope of nitramine and TATP unimolecular initiation. While the TATP-specific part of the training set is limited to unimolecular decomposition data, the chemical variety encountered in the rest of the training set should ensure that ReaxFF gives a reasonable description of secondary reactions, including bimolecular rearrangements. After reevaluating the ReaxFF parameters against this TATP-augmented training set, we obtained a satisfactory agreement between the ReaxFF and QM energies for the relative energies of the reactants, products, intermediates, and transition states observed in the TATP unimolecular decomposition pathway (Figure 3). ReaxFF reproduces most QM energies within 5 kcal/mol (especially those directly related to the TATP initiation reactions). The largest deviation between ReaxFF and QM energies is for $DMCO+2$ acetone+ O_2 , for which the ReaxFF energy (compared to the

parent TATP molecule) is 9.5 kcal/mol higher than the QM energy.

3.2. Comparison of Unimolecular and Condensed-Phase Cookoff Simulations. To establish whether TATP is initiated by a unimolecular reaction or, alternatively, is caused by a multimolecular reaction, we performed a series of MD cookoff simulations on a single TATP molecule and on a TATP solid phase. The TATP solid phase was represented by a periodic TATP crystal supercell containing 32 TATP molecules. These simulations started with a configuration pre-equilibrated at 300 K. Subsequently, the system temperature was raised at a rate of 200 K/ps, reaching a final temperature of 2800 K after 12.5 ps. During these cookoff simulations we found that TATP dissociation is initiated. To obtain meaningful statistics, the single-molecule cookoff simulations were repeated 100 times with different initial atom positions and velocities. The results in Figure 4 show the distribution of product molecules from these 100 independent single-molecule cookoff simulations; Figure 5 shows the distribution of product molecules observed for the condensed-phase TATP cookoff. We observe in both cases that TATP dissociation starts at a system temperature of just over 1300 K. Furthermore, we observe a close similarity in the primary reaction products from the single-molecule and condensed-phase cookoff simulation (acetone, O₂, dimethyldioxacyclopropane, DMDO, and DADP). Indeed, three of these major initial products (acetone, O₂, and DMDO) were predicted by the QM unimolecular decomposition data⁷ (Figure 3). As such, our results strongly indicate that TATP initiation is caused by unimolecular reactions involving a dissociation of the O–O bond. This is plausible, since this is by far the weakest bond in the molecule. To determine the effect of heating rate on our results, we also simulated the condensed-phase TATP cookoff at a 5 times slower rate (40 K/ps). We found that in this case the initiation temperature drops from just over 1300 to 1250 K. After initiation, a product distribution is observed that is very similar to that shown in Figure 5.

In the single-molecule cookoff experiments, we find that acetone, O₂, and DMDO all survive the continued heating to 2800 K, while DADP undergoes further dissociation along channels similar to the parent TATP. No major secondary reaction products are observed. In the condensed-phase simulations, however, we find significant amounts of secondary reactions resulting in reductions in the acetone and O₂ concentration, an almost complete removal of the unstable DMDO molecule and formation of a large range of small molecules, including water and a range of C₁–C₇ hydrocarbons, acids, alcohols, ketones, ethers, and aldehydes (summed as “Others” in Figure 5). We find that in the condensed-phase simulations the TATP molecules roughly remain at their crystallographic positions until the initiation of the chemical events. This is not surprising, as the high heating rate and the fixed cell volume limit the time and volume available for substantial molecular diffusion.

3.3. Extended Cookoff Simulations; O₂ Triplet versus O₂ Singlet. The results in Figures 4 and 5 indicate that a wide range of multimolecular secondary reactions occur in the condensed phase, even though the primary reactions are unimolecular. However, we were concerned that these secondary reactions might be caused by the high final temperatures (2800 K) reached in the simulations producing these results. To further elucidate

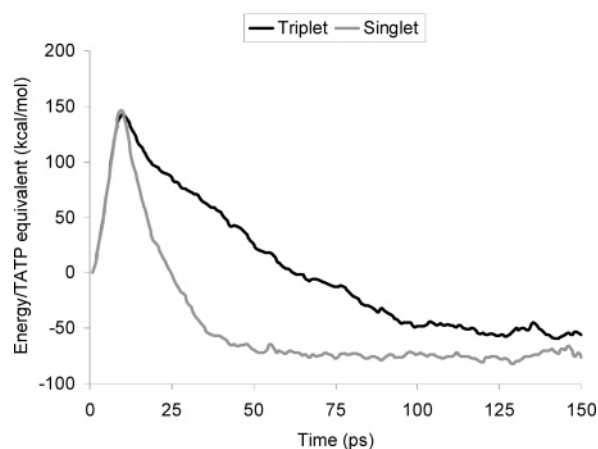


Figure 7. Potential energy observed in the condensed-phase TATP cookoff simulations in which the O₂ bond energy corresponds to either singlet or triplet O₂. The kinetic energy of the system increases from 28 (at $T = 300$ K) to 174 kcal/TATP equivalent (at $T = 1800$ K) during the cookoff simulation in both simulations.

the nature of these secondary reactions at more realistic (and constant) temperatures, we performed a second cookoff simulation. In this simulation, the system was taken from 300 to 1800 K in 7.5 ps (heating rate 200 K/ps), but the temperature was subsequently kept fixed at 1800 K for an additional 142.5 ps. Figure 6a shows the product distribution observed in this simulation. We find results similar to those described in section 3.2:

- (i) The TATP crystal initiates at a temperature of around 1400 K.
- (ii) This results in the formation of acetone, O₂, DMDO, and DADP and a range of minor products, including several radical species.
- (iii) DADP and DMDO rapidly undergo secondary reactions, surviving only for, respectively, 20 and 30 ps.
- (iv) Acetone is far more resistant, and we retain a constant level of almost one acetone for every initial TATP molecule after 150 ps.

The most interesting aspect of the secondary reactions involves the formation and subsequent consumption of O₂. The O₂ concentration reaches a maximum level of about 0.8/TATP after about 20 ps, which corresponds to the time at which all the O₂ producers (TATP and DADP) have disappeared.

In the next 80 ps, O₂ gets consumed in a range of secondary reactions that primarily lead to the formation of large numbers of water molecules and a wide range of small hydrocarbons, acids, ketones, aldehydes, ethers, and alcohols. While the primary reactions are energy-neutral and entropy-driven, these secondary O₂ consumption reactions are exothermic (Figure 7). After 100 ps all O₂ is consumed, and the system energy becomes stable, indicating that chemical equilibrium has been reached (at least for these relatively short time scales).

All simulations described above were performed using the ReaxFF description of the O₂ molecule with a O–O dissociation energy for the triplet ground state of $D_e = 124.9$ kcal/mol, which is close to the experimental value of $D_e = 120.7$ kcal/mol. However, the unimolecular decomposition of TATP is likely to produce a significant amount of singlet O₂⁷ (either $^1\Delta_g$ or $^1\Sigma_g^+$), with an O–O bond of only $D_e = 98.2$ kcal/mol for $^1\Delta_g$ or 83 kcal/mol for $^1\Sigma_g^+$. To investigate where the generation of the less stable singlet O₂, rather than the more stable triplet O₂,

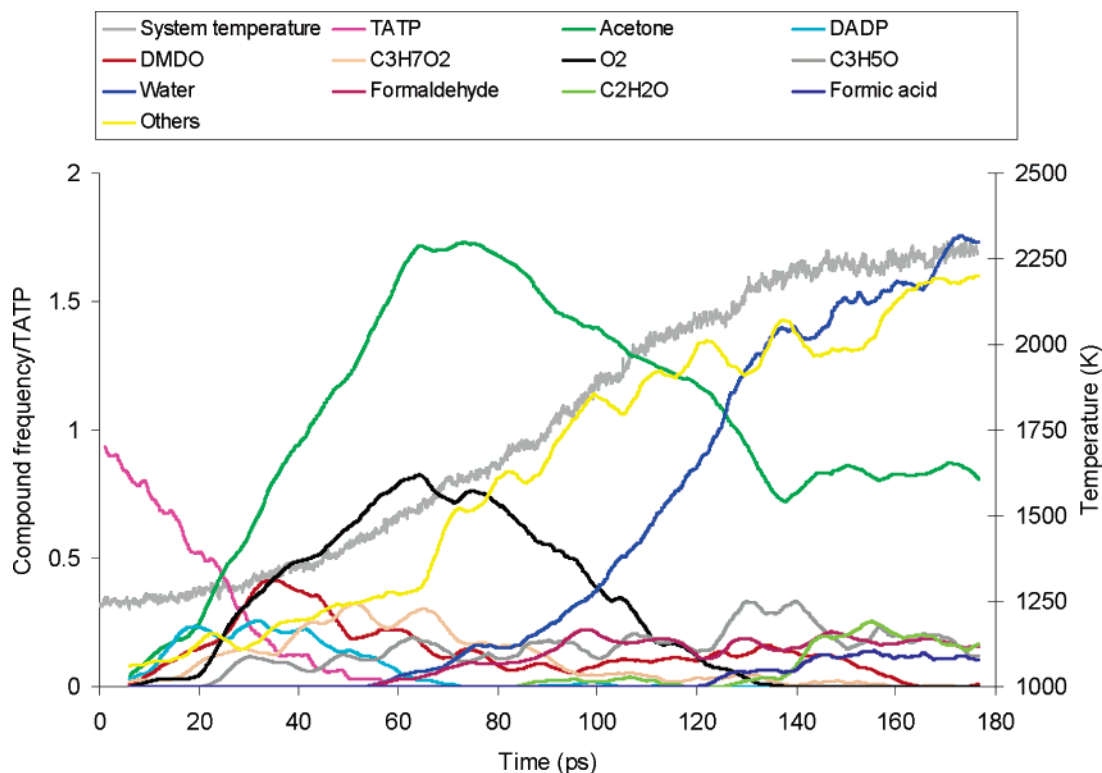


Figure 8. Products observed in the solid TATP NVE simulation initiated at $T = 1250$ K. Only major products are shown explicitly; all minor products are summed in “Others”.

might affect the TATP initiation, we optimized a second set of ReaxFF parameters (ReaxFF^{singlet}), fitted against exactly the same data as the force field employed in the simulations described above but with an O–O double bond dissociation energy in O₂ of 92.5 kcal/mol instead of 124.0 kcal/mol. Since TATP contains single O–O bonds and since ReaxFF allows separate parameters for single, double, and triple bond orders and their bond energies, we were able to implement these modifications in the O₂ bond dissociation energy without significantly affecting the fitting to the remainder of the QM data used to describe the unimolecular TATP dissociation paths (Figure 3).

We then applied ReaxFF^{singlet} in the same cookoff simulation as described previously in this section. The results in Figures 6b and 7 show that the only significant effect resulting from this modification from O₂ triplet to O₂ singlet is to accelerate the rate of the secondary O₂ consumption reactions. With the triplet description we find that O₂ survives until about 100 ps (Figure 6a), but the singlet O₂ is completely consumed after only 30 ps, resulting in a faster production of the secondary reaction products, which are dominated by water. This increase in secondary reaction rate does not change the chemical equilibrium configuration reached after 150 ps. Thus we obtain a virtually similar compound distribution of molecular products, dominated by water, acetone, and a range of small hydrocarbons, acids, ketones, aldehydes, ethers, and alcohols. Also, the overall drop in potential energy during the cookoff simulation is very similar for the O₂ triplet and O₂ singlet cases (Figure 7).

3.4. NVE Simulation. The simulations in sections 3.2 and 3.3 were biased by temperature scaling linked with a fast heating rate. To create a more unbiased simulation of the TATP initiation events, we performed a constant energy (NVE) or adiabatic simulation on the TATP crystal using the triplet O₂

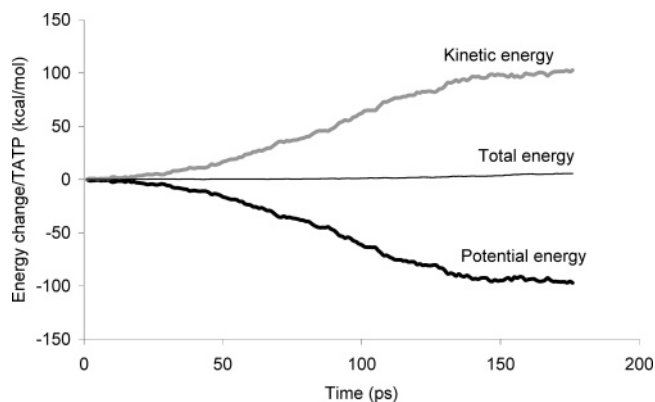


Figure 9. Potential, kinetic, and total energies from the NVE simulation.

ReaxFF. For this simulation we started with the atom positions and velocities equivalent to a system temperature of 1250 K, as generated during the 200 K/ps cookoff simulations from section 3.3, and performed a 180-ps NVE simulation. In the initial configuration no reactions happened and all 32 TATP molecules were still near their original crystallographic positions. This initial temperature was chosen since it is close to the TATP initiation temperature observed during the 200 K/ps solid-phase cookoff experiments (1300 K; Figure 5) and is in line with the initiation temperature observed in the 40 K/ps solid-phase cookoff experiments.

Figure 8 shows the product distribution and system temperature observed during this simulation. These results show that, in agreement with the cookoff experiments, TATP almost immediately begins to dissociate at the initial temperatures and steadily decomposes during the first 60 ps. Until the appearance of the products from the secondary reactions (water and formaldehyde) at $t = 50$ ps, the system temperature does not

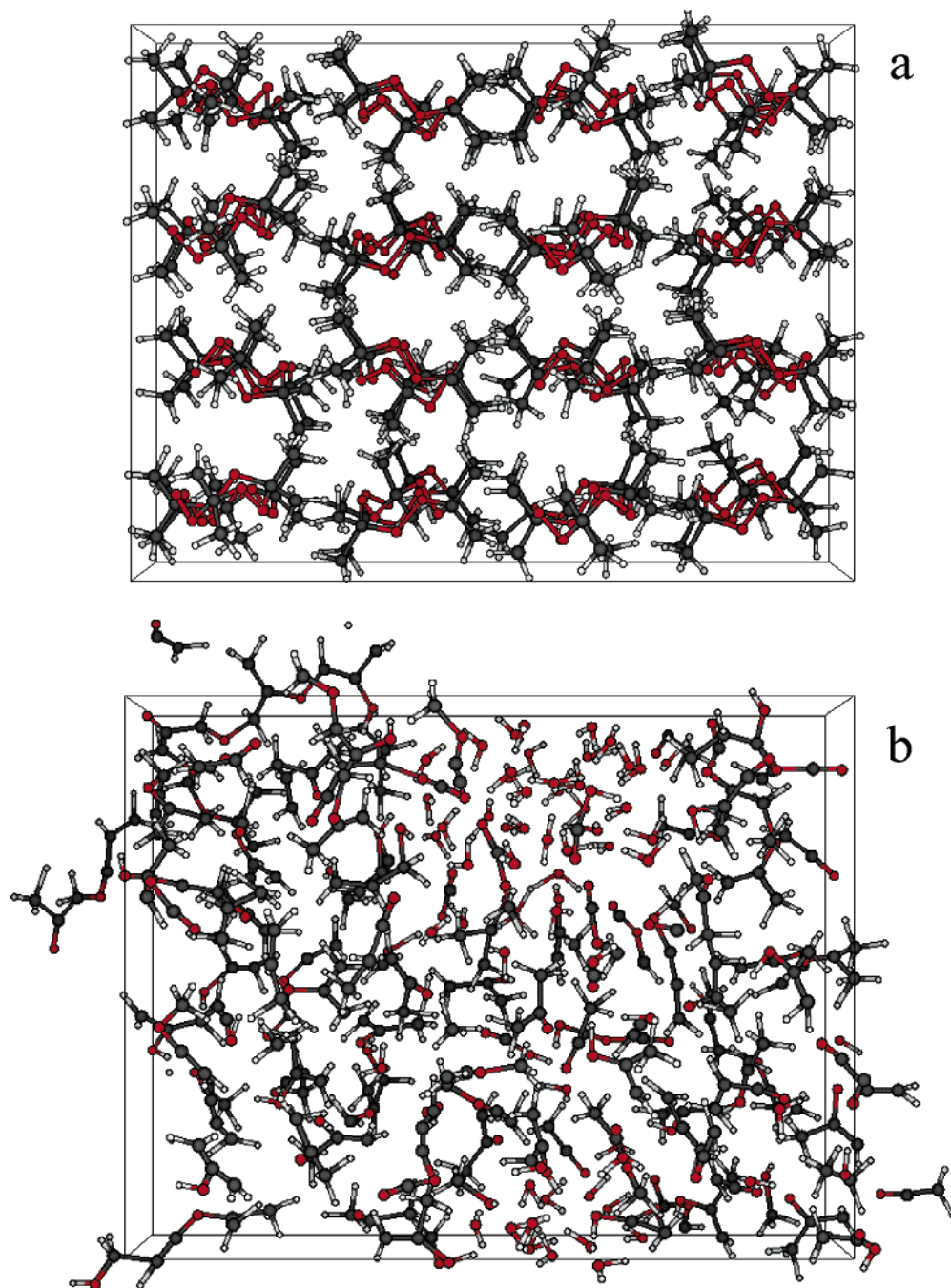


Figure 10. (a) Solid TATP (32 monomers; density = 1.272 kg/dm³) after equilibration at 300 K. (b) System configuration at the end of the NVE simulation ($T = 2300$ K).

rise substantially, indicating that the primary decomposition of TATP is not exothermic. Thus, the later rise in system temperature to $T = 2250$ K at $t = 180$ ps can be attributed to the exothermic secondary reactions. The products observed from primary and secondary reactions in this NVE simulation show very similar trends to those observed from the NVT cookoff simulation (Figure 6a); we see a major primary production of acetone and O₂, followed by a steady consumption of the O₂ during the secondary reactions, leading primarily to water and a range of small hydrocarbons, acids, ketones, aldehydes, ethers, and alcohols. During the NVE simulation the system pressure rises from 2.5 GPa at the initial temperature of 1250 K to a

final pressure of 8 GPa at the final temperature of 2250 K. We find a linear correlation between system temperature and pressure.

Figure 9 shows that the overall reaction leads to a 100 kcal/mol increase/decrease in kinetic/potential energy and demonstrates that the ReaxFF NVE simulation displays very good energy conservation, even during complicated chemical events at high temperatures and pressures.

Figure 10 shows snapshots of the initial TATP crystal configuration at $T = 300$ K and the final NVE system configuration at $T = 2300$ K. Interestingly, the water molecules formed during the secondary reactions seem to cluster together,

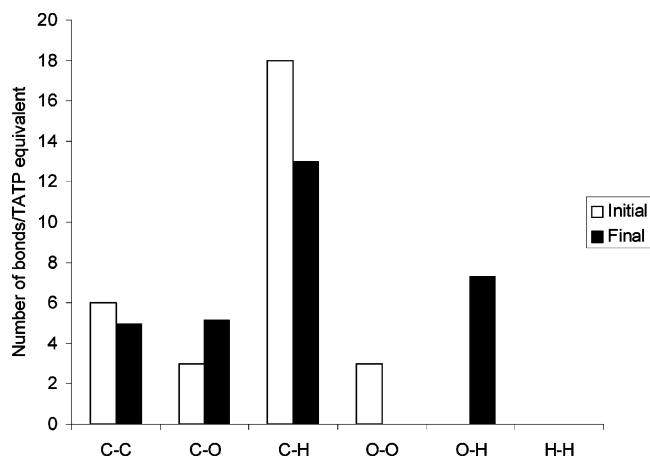


Figure 11. ReaxFF bond distribution for the initial solid TATP and for the final configuration obtained from the NVE simulation after cooling the system to 300 K and depressurization to 1 atm. Only bond orders larger than 0.3 are considered in this analysis.

forming a water bubble surrounded by carbon-containing molecules. While this may be related to a phase separation driven by differences in polarity, it may also indicate that water autocatalyzes water formation, lowering the barriers for the C–H \rightarrow O hydrogen-shift reactions.

These NVE simulations demonstrate that, on the picosecond time scale of our simulations, TATP initiation occurs at relatively low temperatures (<1250 K). This initiation temperature is significantly lower than those observed in ReaxFF simulations on the nitramine RDX crystal,¹² where under similar conditions initiation occurs at around 1500 K. This trend is consistent with the high sensitivity of peroxide-based explosives compared to that of nitramine-based explosives. While we have to bear in mind that the simulations presented here were performed on a highly idealized system, containing no crystal defects, a uniform chemical composition, and only addressing thermally induced initiation, these results indicate that ReaxFF could be part of a computational strategy for predicting high-

energy material sensitivity. All simulations presented here were performed with a nonoptimized single processor code; ongoing work aimed at optimizing and parallelizing the ReaxFF code will allow simulations on substantially larger systems ($>10^6$ atoms), which will enable realistic reactive dynamical simulations of shock waves and crystal defects.

To further analyze the final products obtained from the NVE simulation, we took the final configuration at $T = 2300$ K and cooled it quickly to 300 K and then depressurized the system during an NPT simulation (employing a Berendsen barostat with time constant of 5 ps). By cooling and depressurizing the system, we remove most of the short-lived chemical bonds, thus obtaining a clearer picture of the fragment composition. Figure 11 shows that the chemical structures after the NVE simulation are distinctly different from those observed in the initial TATP crystalline condensed phase. All the weak initial O–O bonds are removed and replaced by stronger C–O (single and double) and O–H bonds. Figure 12 shows a detailed breakdown of the chemical structure of the observed products. We find that nearly all of these products make good chemical sense and contain functional groups whose stability and chemistry are covered by the ReaxFF training set. The only significant exception is the $\text{H}_2\text{C}=\text{C}=\text{O}$ molecule that we observe frequently, which may be an artifact from the ReaxFF description, as we had not included structures with a C=C=O functionality in the ReaxFF training set. We will perform QM simulations on molecules containing this functionality and add these to future ReaxFF training sets. In addition to the wide range of low-mass fragments discussed above we observe some bigger condensation products (mass 100–280 amu), held together by multiple ether linkages.

4. Conclusions

To determine the initial chemical events related to the detonation of TATP, we have extended the ReaxFF reactive force field to reproduce the QM-derived relative energies of the reactants, products, intermediates, and transition states related

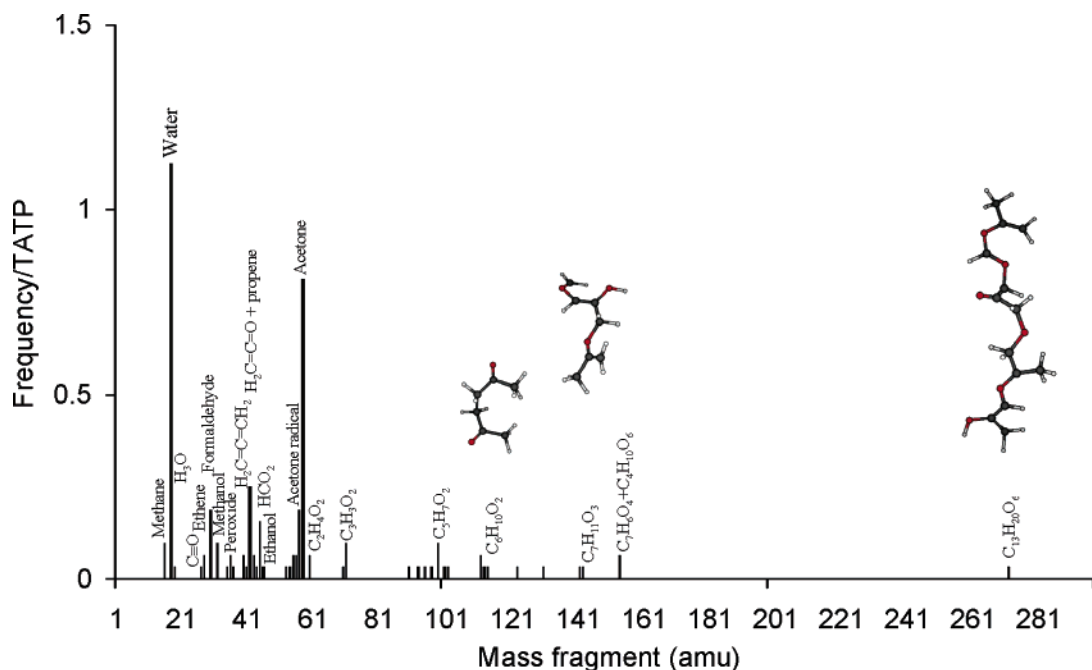


Figure 12. Molecular weights and structures of the fragments obtained from the NVE simulation after cooling to 300 K and depressurizing the system.

to the unimolecular decomposition of TATP. Then we used ReaxFF to perform a series of MD simulations on single-molecule and condensed-phase TATP.

We find that the primary reaction products and average initiation temperature observed in 100 independent unimolecular cookoff simulations match closely with those observed from a TATP condensed-phase cookoff simulation, indicating that unimolecular decomposition dominates the initiation of decomposition in the TATP condensed phase. Furthermore, the reaction products observed in the unimolecular cookoff simulations match closely with those predicted from the QM simulations, validating the ReaxFF description.

Our simulations demonstrate that initiation of condensed-phase TATP is entropy-driven, not enthalpy-driven. Thus the initiation reaction, which leads mainly to formation of acetone, O₂, and several unstable C₃H₆O₂ isomers, is almost energy-neutral. The O₂ generated in the initiation steps is subsequently utilized in exothermic secondary reactions leading to the formation of water and a wide range of small aldehydes, ketones, ethers, and alcohols. We find that the TATP initiation temperature observed in our simulation is significantly lower (by about 300 K) than those observed for the nitramine RDX in similar

simulations (see Strachan et al.¹²). This agrees with the high sensitivity observed for peroxide-based explosives, as compared to that of the nitramine-based materials.

The results presented here were obtained from simulations on a relatively small TATP crystallite (32 monomers) under idealized conditions (uniform heating rate, uniform chemical composition) and as such only address some aspects of the complicated physical and chemical events associated with the initiation and propagation of high-energy materials. However, the results presented here demonstrate that, within the confines of these idealized conditions, ReaxFF provides a reasonable description of the chemical events associated with thermal initiation and, as such, provides a computational framework for studying aspects of the sensitivity of these high-energy materials.

Acknowledgment. This research was supported by funding from ONR and DARPA-PROM (N00014-00-1-0839). The MSC computational facilities were provided by grants from ARO-DURIP and ONR-DURIP. Partial support for this research was obtained from funding by NATO (SFP 980873). We thank the reviewers for their constructive review of this manuscript.

JA052067Y